Journal of Ceramic Processing Research. Vol. 25, No. 4, pp. 557~562 (2024)
(Received 18 April 2024, Received in revised form 14 June 2024, Accepted 14 June 2024)
https://doi.org/10.36410/jcpr.2024.25.4.557

J O U R N A L O F
Ceramic Processing Research

Physical properties and antioxidant activity of ZnO nanoparticles synthesized by *Moringa oleifera* leaf extract at different pH values

Iwan Sugihartono[a,*], Ridha Octa Alhuriyyah Azzahra[a], Nurfina Yudasari[b], Esmar Budi[a], Riser Fahdiran[a], Widyaningrum Indrasari[a], Tan Swee Tiam[c], Rahmat Setiawan Mohar[b], Isnaeni[b], Djoko Triyono[d], Fera Kurniadewi[e] and Agus Setyo Budi[a]

[a]*Program Studi Fisika, FMIPA, Universitas Negeri Jakarta, Jalan Rawamangun Muka no. 01, Jakarta Timur, 13220, Indonesia.*
[b]*National Research and Innovation Agency, KST BJ Habibie, South Tangerang, 15314 Indonesia*
[c]*School of Energy and Chemical Engineering, Xiamen University Malaysia, Selangor Darul Ehsan 43900, Malaysia*
[d]*Departemen Fisika, FMIPA, Universitas Indonesia, Kampus Baru UI, Depok, 16424, Indonesia*
[e]*Program Studi Kimia, FMIPA, Universitas Negeri Jakarta, Jalan Rawamangun Muka no. 01, Jakarta Timur, 13220, Indonesia.*

We have demonstrated green synthesis of ZnO nanoparticles using *Moringa oleifera* leaves (*Mor*-ZnO NPs) extract by co-precipitation method under 450°C for 2 hours with different pH-5, pH-7, and pH-8. The physical properties (i.e. structural, morphology, and absorbance) have been analyzed using X-ray diffraction (XRD) measurement, scanning electron microscopy (SEM), and ultraviolet-visible (UV-Vis) spectrophotometer. Furthermore, to investigate the functional group and antioxidant activity we performed Fourier transform infra-red (FTIR) analysis and 2,2-*diphenyl*-1-*picrylhydrazyl* (DPPH) assay. Structurally, all samples possess polycrystalline hexagonal wurtzite structure. Morphologically, the pH values affect the morphology of *Mor*-ZnO NPs. Optically, the *Mor*-ZnO NPs with pH-8 have strong absorption in the range of short ultraviolet (200-280 nm). We predict that the basic pH value on green synthesize of *Mor*-ZnO NPs tune the near band edge absorption (NBA), which relates to the recombination of the free excitons. Whereas, based on the FTIR spectra analysis, the Zn-O stretching can be identified at 442.67 cm^{-1}, 458.67 cm^{-1}, and 442.67 cm^{-1} for *Mor*-ZnO NPs with the pH-5, pH-7, and pH-8, respectively. According to DPPH assay, the Mor-ZnO NPs with pH-8 at 200 mg/ml has higher inhibition rate (67.7%). Hence, we believed that the Mor-ZnO NPs are potential antioxidants.

Keywords: Green-synthesis, *Mor*-ZnO NPs, pH, Physical properties, Antioxidants.

Introduction

In the last three decades, ZnO as a nanomaterial semiconductor has still become an interesting research subject due to the wide direct band gap energy and strong binding exciton energy of 3.37 eV and 60 meV, respectively [1, 2]. Instead of that, it has high chemical stability, high electrochemical coupling coefficient, broad range of radiation absorption, high photostability, good transparency, high electron mobility, strong room temperature luminescence, high thermal and mechanical stability at room temperature, and broad range of radiation absorption [3, 4]. Hence, ZnO is believed to be a potential candidate nanomaterial for broad applications in nanotechnology [5]. Moreover, Raha et al. believed that as the second abundant metal oxide after iron, the ZnO is inexpensive, safe, and easy to be prepared in any forms [3].

*Corresponding author:
Tel : +62-021-4890856
Fax: +62-021-4890856
E-mail: iwan-sugihartono@unj.ac.id

Recently, the manipulation of atoms at the nanoscale has become of great interest. Nanoparticles (NPs) with a size in the range between 1 nm to 100 nm potentially offer numerous applications in wide areas such as biomedicine, optoelectronics, catalysts, etc. [6]. Moreover, many reports have shown that the physical properties such as structure, shape, size, and morphology of ZnO nanoparticles (NPs) strongly depend on synthesize methods [3].

Most ZnO NPs have been demonstrated by bottom-up approaches such as evaporation, chemical vapor deposition, chemical bath deposition, sol-gel method, precipitation, etc [7-9]. Compared with other methods, the synthesis method of ZnO NPs using the plant extract belongs to the bottom-up approach, which offers simplicity, no additional chemicals, an environmentally friendly, reliable method, low toxicity, and low cost [10]. As well known, the plant extract consists of a phytochemical compound that is naturally present in seeds, flowers, leaves, roots, and peels and can be used for the biological reduction of metal ions [11, 12].

Sondergaard et al. report that the crystallinity, size, and morphology of ZnO NPs depend on the synthesis

conditions i.e., temperature, precursor, and pH [13]. Therefore, the synthesis of ZnO NPs using biological techniques has been carried out using plant extracts such as Momordica charantia, Amaranthus caudatus, Abutilon indicum, Clerodendrum infortunatum and Clerodendrum inerme, Azaridacta intica, Tabernaemontana divaricata, Kalopanax septemlobus, Conyza Canadensis, Glycosmis pentaphylla, and Cogtus igneus [14]. Vinotha et al. reported that the ZnO NPs synthesized by Cogtus igneus extract showed promising antibacterial and biofilm inhibitory effects against the pathogenic bacteria Streptococcus mutans, Lysinibacillus fusiformis, Proteus vulgaris, and Vibrio parahaemolyticus [14]. Nevertheless, compared to the other leaves, Moringa Oleifera contains very important bioactive compounds (i.e. vitamins, flavonoids, phenolic acids, and glucosides) for improving biomedicine [11]. Matinise et al. reported that the ZnO NPs could be obtained by biosynthesis-based Moringa Oleifera leaf extract as a chelating agent for Zn^{2+} [15]. Furthermore, ZnO NPs produced by biosynthesis have better antioxidant activity than chemical processes [16]. As suggested by Gherbi et al., the formation of ZnO NPs during biosynthesis is strongly influenced by the pH of the solution [17]. Moreover, Alias et al. reported that the ratio of H^+ or OH^- influence the metal-oxygen bonds, hence, plays an important role to control shape and size of ZnO [18].

In this paper, the green synthesis of Mor-ZnO NPs has been demonstrated using co-precipitation methods with a temperature of 450ºC for 2 hours with different pH values (5, 7, and 8). Precipitation has been chosen due to its offer of low cost, simple method, scalable, and has been used to synthesize various kinds of ZnO nanostructures [19].

Experimental Methods

Preparation of Moringa oleifera leaves extract

The leaves of Moringa oleifera were produced by local farmers in the northern Bekasi region, West Java, Indonesia. The leaves of Moringa oleifera were washed with deionized water to remove impurities from the leaves. The cleaned leaves of the Moringa oleifera plant were then dried at room temperature (32°C) for 3 to 5 days. Dry leaves of Moringa oleifera were ground into a powder using a blender.

The extract used for the reduction of zinc ions (Zn^{2+}) to ZnO-NPs was prepared by adding 20 grams of powder leaves into a 200 mL beaker along with 100 mL of deionized water at 60°C for 20 minutes under a hot plate magnetic stirrer and a dark light was given. A yellow aqueous solution was obtained. The extract was allowed to cool at room temperature and filtered with Whatman filter paper to avoid organic solid residues. The Moringa oleifera leaf extract is then diluted by adding deionized water. The concentration ratio of the extract to deionized water is 1:10, creating a liquid Moringa oleifera extract.

Biosynthesis of ZnO NPs

The 20 mL of Moringa oleifera liquid leaf extract was placed in a 150 mL beaker and heated to 70°C using a magnetic stirrer with a hot plate. When the extract temperature reached 70 to 80°C, 2.195 grams of zinc acetate dihydrate [$Zn(CH_3COOH)_2 \cdot 2H_2O$] was added as a precursor. After 20 minutes, a NaOH solution is added dropwise for adjusting the pH values of the solution from 5 (acidic), 7 (neutral) to 8 (alkaline). The mixture is heated under constant temperature of 80°C and stirring constantly, until the color of the mixture changes from golden yellow to pale yellow. The mixture is then left to stand for an hour, whereby a white-milky precipitate forms. The resulting pure white precipitate is washed three times with de-ionized (DI) water to remove acetate followed by centrifuging at 1000 rpm for 10 minutes. To evaporate the solvent and remove the organic residue, the precipitate is then dried in an oven at a temperature of 100°C for 4 hours. Finally, we obtained the ZnO NPs by annealing the dried precipitated in an oven at a temperature of 450°C for two hours.

Results and Discussion

The X-ray diffraction (XRD) measurement (with CuKa radiation PAN-analytical) has been performed to characterize structural properties of *Mor*-ZnO NPs. Fig. 1 shows XRD pattern of the *Mor*-ZnO NPs with pH-5, pH-7, and pH-8. We observed nine crystal planes (Miller indices) of *Mor*-ZnO NPs with the hkl are (100), (002), (101), (102), (110), (103), (200), (112), and (201). As seen in Fig. 1, the *Mor*-ZnO NPs for all pH condition have three intense peaks corresponding to the (100), (002), and (101) planes. As observed, there is no other phase besides ZnO. Moreover, based on the *Inorganic Crystal Structure Database* (ICSD) number #98-018-

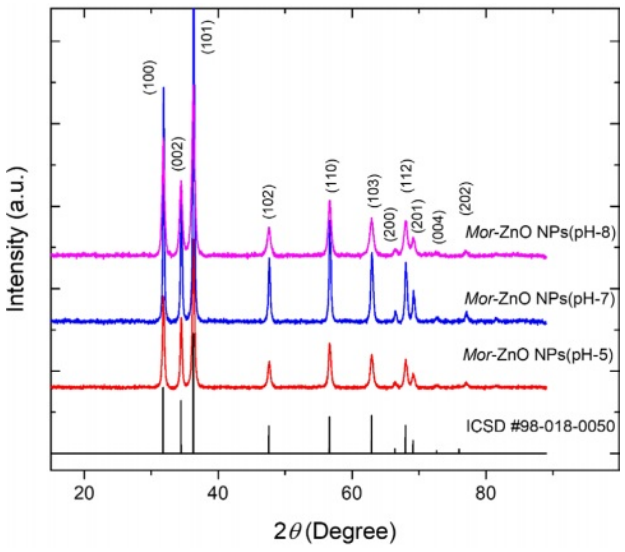

Fig. 1. XRD pattern of the *Mor*-ZnO NPs with pH-5, pH-7, and pH-8.

0050, all the samples possess polycrystalline hexagonal wurtzite structure. Normally, the ZnO NPs cannot be formed perfectly under acidic conditions (pH-5) due to few concentration of OH^- ions. Meanwhile, for the neutral conditions (pH-7), there is equivalently number of reaction OH^- ions and H+ ions [18]. However, according to the XRD pattern, we believed the ZnO NPs grown by green synthesis under acidic and neutral pH condition is highly crystalline due to annealing process [20]. Further analyses, we then calculated crystallite size by using Debye-Scherer equation [6] and structural parameters of the *Mor*-ZnO NPs.

As summarized in the Tables 1-3, the lattice parameters do not show any significant change, hence, the ratio of c/a value for all samples of *Mor*-ZnO NPs about ~1.60 which in good agreement with the ICSD. The diffraction angle of *Mor*-ZnO NPs is not significantly shifted for all the plane of reflections. Meanwhile, the full width of half maximum (FWHM) corresponds to the crystallite size and micro strain of the samples. Further calculations, the average crystallite size of *Mor*-ZnO NPs for pH-5, pH-7, pH-8 are 52.57 nm, 67.23 nm, 64.42 nm, respectively. Moreover, the average micro strain of *Mor*-ZnO NPs for pH-5, pH-7, pH-8 are 0.22%, 0.15%, and 0.17%, respectively. Based on these results, the pH value affects the crystalline properties of *Mor*-ZnO NPs.

Table 1. The structural parameters of *Mor*-ZnO NPs with pH-5.

(hkl)	2θ(°)	FWHM (°)	a=b (Å)	c (Å)	c/a	d_{hkl} (Å)	Volume (Å)	Crystallite size (nm)	Micro-strain (%)
(100)	31.789	0.117	3.25	5.205	1.602	2.814	47.61	94.719	0.149
(002)	34.478	0.301	3.25	5.205	1.602	2.601	47.61	31.855	0.408
(101)	36.262	0.167	3.25	5.205	1.602	2.477	47.61	60.886	0.203
(102)	47.579	0.234	3.25	5.205	1.602	1.911	47.61	43.43	0.22
(110)	56.625	0.301	3.25	5.205	1.602	1.626	47.61	34.592	0.235
(103)	62.883	0.335	3.25	5.205	1.602	1.478	47.61	32.001	0.231
(112)	67.942	0.167	3.25	5.205	1.602	1.379	47.61	70.511	0.098

Table 2. The structural parameters of *Mor*-ZnO NPs with pH-7.

(hkl)	2θ(°)	FWHM (°)	a=b (Å)	c (Å)	c/a	d_{hkl} (Å)	Volume (Å)	Crystallite size (nm)	Micro-strain (%)
(100)	31.839	0.184	3.25	5.205	1.602	2.81	47.61	53.932	0.149
(002)	34.509	0.15	3.25	5.205	1.602	2.599	47.61	68.699	0.189
(101)	36.329	0.167	3.25	5.205	1.602	2.477	47.61	60.896	0.189
(102)	47.631	0.134	3.25	5.205	1.602	1.909	47.61	83.214	0.115
(110)	56.675	0.117	3.25	5.205	1.602	1.624	47.61	104.346	0.078
(103)	62.922	0.368	3.25	5.205	1.602	1.477	47.61	28.996	0.255
(112)	68.008	0.167	3.25	5.205	1.602	1.379	47.61	70.542	0.098

Table 3. The structural parameters of *Mor*-ZnO NPs with pH-8.

(hkl)	2θ(°)	FWHM (°)	a=b (Å)	c (Å)	c/a	d_{hkl} (Å)	Volume (Å)	Crystallite size (nm)	Micro-strain (%)
(100)	31.805	0.117	3.248	5.202	1.602	2.813	47.52	94.721	0.148
(002)	34.482	0.167	3.248	5.202	1.602	2.601	47.52	60.59	0.214
(101)	36.314	0.117	3.248	5.202	1.602	2.477	47.52	95.789	0.129
(102)	47.648	0.134	3.248	5.202	1.602	1.909	47.52	83.22	0.115
(110)	56.652	0.368	3.248	5.202	1.602	1.625	47.52	28.081	0.289
(103)	62.889	0.268	3.248	5.202	1.602	1.478	47.52	40.467	0.183
(112)	68.02	0.234	3.248	5.202	1.602	1.378	47.52	48.161	0.143

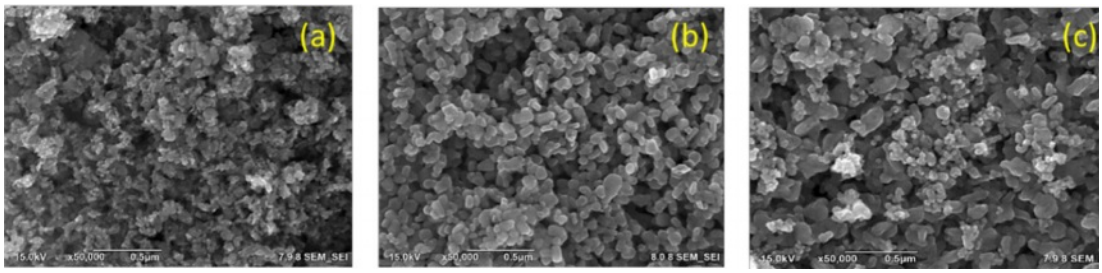

Fig. 2. The SEM images of *Mor*-ZnO NPs with pH-5, pH-7, and pH-8.

Gherbi et al. believed that the crystallite size reduces by the increasing pH value [17]. To the best of our knowledge, the concentration of OH^- ions affect the particle size. Then, by increasing pH, the nucleation rate higher and the particle size would decrease. Furthermore, others reported that the increasing pH value will enhance the crystallinity of ZnO NPs [21].

Scanning electron microscopy (SEM) was performed to observe the morphology of the powder of *Mor*-ZnO NPs with different pH. Fig. 2 shows the SEM images of *Mor*-ZnO NPs with pH-5, pH-7, and pH-8. As seen in the figure, the morphology of the powder of *Mor*-ZnO NPs with pH-5 indicated the strong agglomeration and the nanoparticles dimension smaller than others. Further investigation, to assess the elemental composition of *Mor*-ZnO NPs with pH-5, pH-7, and pH-8, the energy dispersive x-ray (EDX) was performed. As confirmed, there are two elements i.e. Zn and O with no other elements related to impurities. Table 4 is the summary of the compositional elements of Mor-ZnO NPs with pH-5, pH-7, and pH-8. As seen in Table 4, both atomic and weight percentage of Zn increase by the pH values. Meanwhile, the oxygen composition of ZnO tends to decrease by the increasing pH values. We believed that the pH value affects the hydrolysis and condensation reactions during nucleation process. Hence, the elemental composition and morphology depend on the amount of H^+ or OH^- ions presented during the green synthesis process [17].

Figure 3 shows the absorbance of Moringa oleifera leaf extract and *Mor*-ZnO NPs with different pH. As seen in the figure, *Mor*-ZnO NPs with pH-8 have strong absorption in the range of short ultraviolet (200-280 nm) compared to *Mor*-ZnO NPs with pH-5 and pH-7. We predict that the strong absorption in the range of ultraviolet (UV) *Mor*-ZnO NPs with pH-8 relates with the ZnO purity, which the intensity significantly increased in the basic condition. Moreover, oxygen controlled the availability to form zinc hydroxide. As result, we observed the absorption due to excitation electrons from the valence to conduction band (excitonic absorption) is stronger than the deep level absorption (DLA). According to our results, the processing condition (pH value) can tune the near band edge absorption (NBA), which relates to the recombination of the free excitons [22]. Hence, we believed that the *Mor*-ZnO NPs can be used as UV light emitting diode (UV-LED).

Figure 4 shows the Fourier Transform Infrared (FTIR) spectra to observe the functional groups of *Mor*-ZnO NPs which synthesize by the different pH values. To the best of our knowledge, *Moringa oleifera* has two

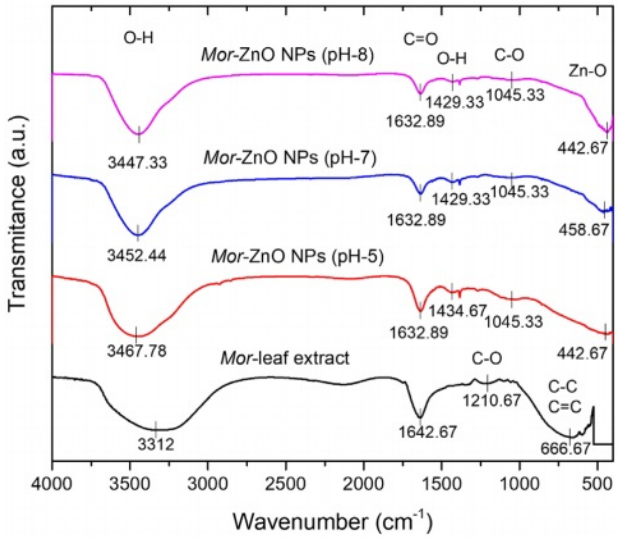

Fig. 3. FTIR spectra of *Moringa oleifera* leaf extract and *Mor*-ZnO NPs with different pH-5, pH-7, and pH-8.

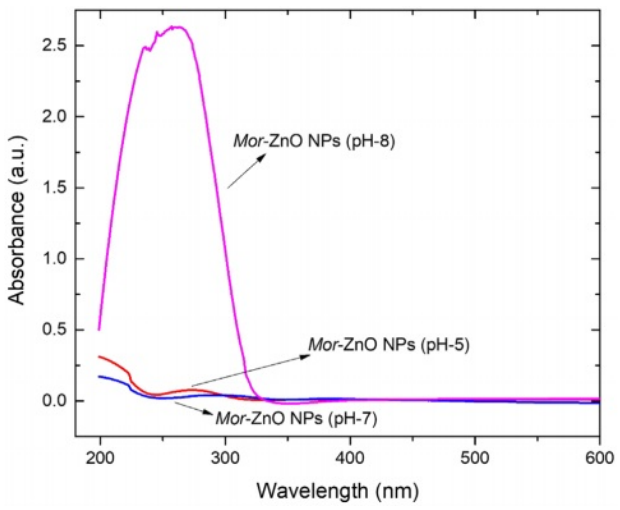

Fig. 4. Absorbance spectra of *Mor*-ZnO NPs with different pH-5, pH-7, and pH-8.

Table 4. The compositional elements of Mor-ZnO NPs with pH-5, pH-7, and pH-8.

	Mor-ZnO NPs					
	pH-5		pH-7		pH-8	
	Zn	O	Zn	O	Zn	O
at.%	49.7	50.3	53.3	46.7	50.1	49.9
wt.%	80.1	19.9	82.4	17.6	80.4	19.6

Table 5. The antioxidant activity of *Mor*-ZnO NPs with pH-5, pH-7, and pH-8.

Mor-ZnO NPs (μg/ml)	% of Inhibition		
	pH-5	pH-7	pH-8
50	20.85	13.05	26.35
100	32.55	42.4	51.25
200	42	52.6	67.7

important compounds i.e., flavonoids and phenolic acids which have an important role in the reduction process for synthesizing *Mor*-ZnO NPs. According to the FTIR spectra of *Mor*-ZnO NPs in the spectral range of 400 to 4000 cm^{-1} as depicted in the Fig. 4, we observed bands in the range of ~632 to 416 cm^{-1} which is indicating stretching mode of vibration (Zn-O) from *Mor*-ZnO NPs. Moreover, we observed the peaks of Zn-O stretching mode from *Mor*-ZnO NPs with the pH-5, pH-7, and pH-8 at 442.67 cm^{-1}, 458.67 cm^{-1}, and 442.67 cm^{-1}, respectively. As seen in Fig. 4, the Zn-O stretching of *Mor*-ZnO NPs (pH-8) has an intense peak at 442.67 cm^{-1}.

An antioxidant is a compound which can prevent the cells from the damage of reactive oxygen species. Natural antioxidants have the potential ability to control diseases and improve human health [14]. To determine the antioxidant activity of *Mor*-ZnO NPs with pH-5, pH-7, and pH-8 we have demonstrated DPPH assay. Table 5 is the summary of the DPPH assay to observe the antioxidant activity of *Mor*-ZnO NPs with pH-5, pH-7, and pH-8. Our results show that the inhibition rate of *Mor*-ZnO NPs for each concentration increases with the pH values. Furthermore, we found that 200 *m*g/ml of *Mor*-ZnO NPs with pH-8 have a higher inhibition rate (67.7%) than other samples. Hence, we believed that the *Mor*-ZnO NPs are potentially acting as an antioxidant which originates from the presence of proteins and amino acids along with other phytochemicals constituents [23]. However, detailed observation of Mor-ZnO NPs to obtained highest inhibition still needs to be established.

Conclusions

In conclusion, the green synthesize of *Mor*-ZnO NPs have been demonstrated by co-precipitation method with different pH under 450°C for 2 hours. The XRD pattern confirmed that all the *Mor*-ZnO NPs have polycrystalline hexagonal wurtzite structure. The SEM images showed that all the *Mor*-ZnO NPs agglomerated with different unit sizes. The FTIR spectrum in the range of ~632 to ~416 cm^{-1} indicate stretching mode (Zn-O) of *Mor*-ZnO NPs. The higher pH will cause the nucleation rate and the purity of *Mor*-ZnO NPs to be higher than other samples. As results, the *Mor*-ZnO NPs with pH-8 have strong absorption in the range of short ultraviolet (200-280 nm).

Acknowledgement

The authors thank the hibah Penelitian Fundamental Reguler DRTPM nomor kontrak 24/UN39.14/PG.02.00. PL/VI/2023 for the financial support.

References

1. S. Iwan, V. Fauzia, A.A. Umar, and X.W. Sun, AIP Conf. Proc 1729 (2016) 020031.
2. S.T. Tan, X.W. Sun, J.L. Zhao, S. Iwan, Z.H. Cen, T.P. Chen, J.D. Ye, G.Q. Lo, D.L. Kwong, and K.L. Teo, Appl. Phys. Lett 93 (2008) 013506.
3. S. Raha and M. Ahmaruzzaman, Nanoscale Adv 4 (2022) 1868-1925.
4. D. Sogets, J. Gradl, R.K. Taylor, V. Vassilev, and W. Peukert, ACS Nano 3[7] (2009) 1703-1710.
5. Z.L. Wang, ACS Nano 2[10] (2008) 1987-1992.
6. S. Mirza, A.A. Hussaini, G. Öztürk, M. Turgut, T. Öztürk, O. Tugay, D. Ulukuş, and M. Yildirim, Inorg. Chem. Commun 155 (2023) 111124.
7. H.A. Jabri, M.H. Saleem, M. Rizwan, I. Hussain, K. Usman, and M. Alsafran, Life 12[4] (2022) 594.
8. F.K. Konan, B. Hartiti, and B. Aka, J. Ceram. Process. Res 20[4] (2019) 372-378.
9. J. Moghaddam and S. Mollaesmail, J. Ceram. Process. Res 14[4] (2013) 459-462.
10. S.S. Salem and A. Fouda, Biol. Trace Elem. Res 199 (2021) 344-370.
11. I. Ngom, B.D. Ngom. J. Sackey, and S. Khamlich, Mater. Today: Proc 36[2] (2021) 526-533.
12. H.R. Vasanthi, N. ShriShrimal, and D.K. Das, Curr. Med. Chem. 19[14] (2012) 2242-2251.
13. M. Sondergaard, E.D. Bojesen, M. Christensen, and B. B. Iversen, Cryst. Growth Des 11[9] (2011) 4027-4033.
14. V. Vinotha, A. Iswarya, R. Thaya, M. Govindarajan, N.S. Alharbi, S. Kadaikunnan, J.M. Khaled, M.N. Al-Anbr, and B. Vaseeharan, J. Photochem. and Photobiol. B 197 (2019) 111541.
15. N. Matinise, X.G. Fuku, K. Kaviyarasu, N. Mayedwa, and M. Maaza, Appl. Surf. Sci 406 (2017) 339-347.
16. K. Velsankar, A. Venkatesan, P. Muthumari, S. Suganya, S. Mohandoss, and S. Sudhahar, J. Mol. Struct 1255 (2022) 132420.
17. B. Gherbi, S.E. Laouini, S. Meneceur, A. Bouafia, H. Hemmami, M.L. Tedjani, G. Thiripuranathar, A. Barhoum, and F. Menaa, Sustainabillity 14[18] (2022) 11300.
18. S.S. Alias, A.B. Ismail, and A.A. Mohamad, J. Alloys. Compd. 499[2] (2010) 231-237.
19. S. Iwan, D. Dianisya, R. Fahdiran, Isnaeni, E. Budi, A.

B. Susila, and E. Handoko, J. Ceram. Process. Res 20[5] (2019) 518-521.
20. A.K. Zak, M.E. Abrishami, W.H.A. Majid, R. Yousefi, and S.M. Hosseini, Ceram. Int 37[1] (2011) 393-398.
21. J.H. Koo and B.W. Lee, J. Ceram. Process. Res 18[2] (2017) 156-160.
22. I. Sugihartono, S.T. Tan, A. Arkundato, R. Fahdiran, Isnaeni, E. Handoko, S. Budi, and A.S. Budi, Mat. Res 26 (2023) 0499.
23. D. Rehana, D. Mahendiran, R.S. Kumar, and A.K. Rahiman, Bioprocess Biosyst. Eng 40 (2017) 943-957.